Some Aspects of the Ozone-Depletion Problem in the Stratosphere

ROOP N. GUPTA* AND WILLIAM L. GROSE†
NASA Langley Research Center, Hampton, Va.

A preliminary investigation of O_3 depletion by NO_x in the exhaust of an SST wake is presented. Initial calculations were made using a model employing a two-step chemistry mechanism consisting of an NO_x catalytic cycle and assuming total NO_x and the ratio NO/NO_2 to be conserved. The analysis includes diffusion and the effect of inhomogeneous mixing. The reaction rate constants used are those recommended for use in the Climatic Impact Assessment Program. The results indicate O_3 depletion in the wake much less severe than reported in earlier investigations which used a much larger reaction rate constant. Subsequent investigation revealed, however, that even the current O_3 depletion rates appear too large. This situation occurs due to the fact that atomic oxygen, needed to sustain the catalytic cycle, is depleted at unrealistically higher rates than can be produced by the photodissociation of NO_2 and O_3 to satisfy the restrictive assumption of NO conservation. Because of the apparent deficiencies in the two-step chemical model, a model is presented with a more realistic chemical mechanism without the requirement for NO conservation. The model includes water vapor and nitric acid production reactions as well as the NO_x catalytic cycle. Although diffusion is not treated, the more complete chemical model provides interesting insight into the O_3 depletion problem. The results indicate that total NO_x and initial NO/NO_2 ratio play an important role in determining O_3 depletion. Furthermore, only in the case of rather extreme concentrations of water vapor or unrealistically large photolysis rates is there any significant conversion of NO_x to HNO_3.

Nomenclature

c_i = concentration of ith chemical species
J_i = photodissociation constant of ith chemical species
K_j = reaction rate constant for jth reaction
L = local integral scale length
M = unreactive chemical species
Ri = Richardson number
t = time
T = temperature
u = longitudinal velocity
w = vertical velocity
Z = vertical distance
Λ = integral (or computational) scale
σ = standard deviation

Subscript

o = initial value

Superscripts

$\bar{}$ = mean component
$'$ = fluctuating component

Introduction

IN a recent publication, Hilst et al.[1] proposed the following approximate mechanism (for the sunlit sky)

$$NO + O_3 \xrightarrow{K_1} NO_2 + O_2 \qquad K_1 = 0.5 \text{ ppm}^{-1} \text{ sec}^{-1} \tag{1}$$

$$NO_2 + O \xrightarrow{K_2} NO + O_2 \tag{2}$$

to investigate the possible depletion of atmospheric O_3 by NO_x in the post-vortex SST exhaust plume at 20 km altitude. The analysis is predicated on the assumptions $NO + NO_2$ = constant, and NO/NO_2 = constant. These assumptions imply that the replenishment of NO by Eq. (2) is not limited by the availability of O which is produced primarily by photolysis of NO_2 and O_3. Production of O_3 within the plume has also been neglected. The results of this investigation indicate the possibility of substantial O_3 depletion and a resultant "ozone hole" in the wake.

The present investigation has a three-fold purpose: a) to perform the calculations of Ref. 1 with $K_1 = 0.6877 \times 10^{-2}$ ppm^{-1} sec^{-1} [as adopted by the chemistry panel of Climatic Impact Assessment Program (CIAP)[2]]. The value of K_1 employed in Ref. 1 is a factor of 70 larger as compared with the value employed here. The smaller value of K_1 should reduce the severity of the O_3 depletion and the resultant "ozone-hole"; b) to examine the production rate of O from NO_2 and O_3 photolysis to determine if sufficient O is present to make the assumption $d(NO)/dt = 0$ (made in Ref. 1) valid; and c) to investigate the role of certain parameters controlling O_3 destruction using a more realistic chemical model and to emphasize the importance of acquiring experimental measure-

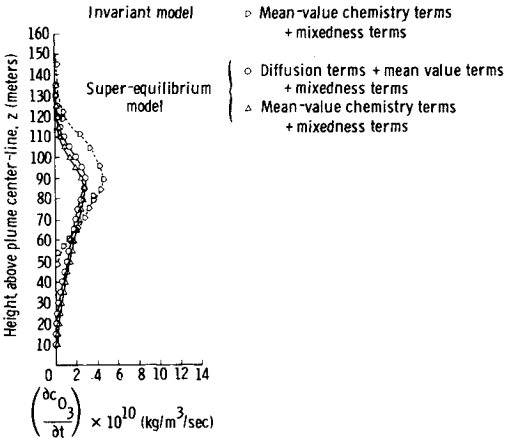

Fig. 1 Vertical profiles of the local depletion rate of O_3 at 150 sec from the start of post-vortex period (with $K = 0.5$ ppm^{-1} sec^{-1}).

Received May 17, 1974; revision received October 29, 1974.
Index categories: Thermochemistry and Chemical Kinetics; Jets, Wakes, and Viscid-Inviscid Flow Interactions.

* NASA-ODU Research Scientist, Space Applications and Technology Division; presently Assistant Professor, Aeronautical Engineering Department, Indian Institute of Technology, Kanpur, India. Member AIAA.
† Aeronautical Research Scientist, Space Applications and Technology Division. Member AIAA.

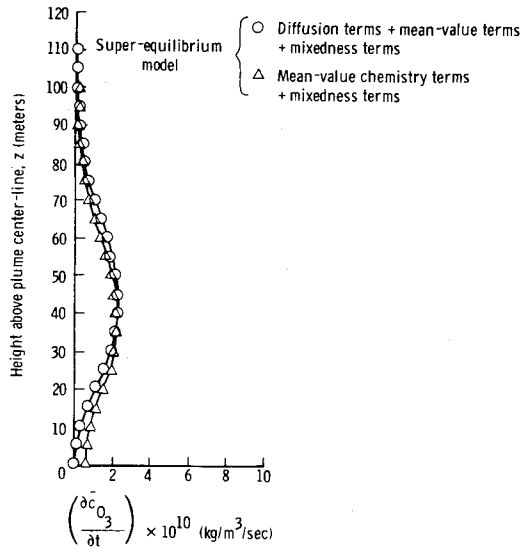

Fig. 2 Vertical profiles of the local depletion rate of O_3 at 150 sec from the start of post-vortex period (with $K = 0.6877 \times 10^{-2}$ ppm^{-1} sec^{-1}).

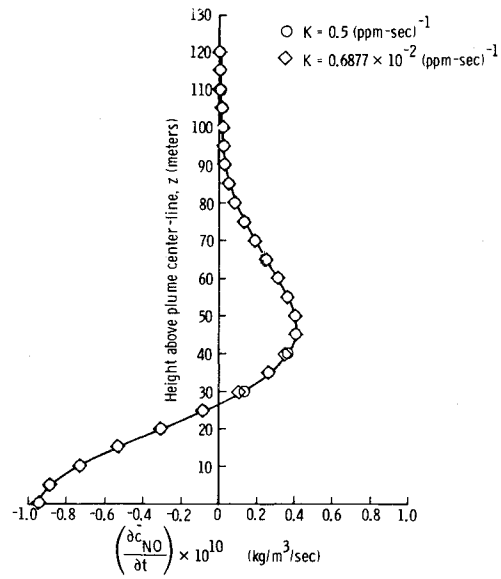

Fig. 4 Vertical profiles of the depletion rate of NO at 150 sec from the start of post-vortex period.

ments of those parameters. Furthermore, the possible role of HNO_3 production as a sink for NO_x can be studied.

Analysis

The calculations performed‡ here are identical to those of Ref. 1 for a "superequilibrium" turbulence field except that the value of reaction rate constant K_1 employed here is 0.6877×10^{-2} ppm^{-1} sec^{-1} rather than 0.5 ppm^{-1} sec^{-1} (used in Ref. 1). The lower value results in a substantial effect on both the O_3-depletion rate and its number density as shown in Figs. 1–3. Figures 1 and 2 show that the maximum O_3-depletion rate is at least 20% smaller than the Hilst et al. prediction (with turbulent diffusion and mixedness terms) when the smaller value of K_1 recommended by the CIAP panel is used. Also, the maxima of the depletion-rate curve moves closer to the plume centerline. The effect of reducing K_1 on O_3 number-density is even more pronounced as evidenced by Fig. 3. At a distance of 80 m above the plume centerline, the lower K_1 results in larger

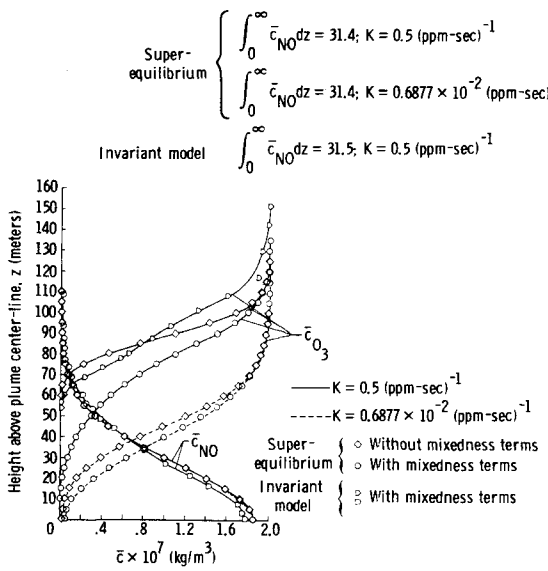

Fig. 3 Vertical profiles of the mean concentration of O_3 and NO at 150 sec from the start of post-vortex period.

‡ Details of the turbulence field, initial NO and O_3 profiles are given in Appendix A. (See also Refs. 1 and 3.)

O_3 number density by approximately 75%. Thus the destruction of O_3 by NO proceeds at a much slower rate than previously calculated which in turn may permit more ambient O_3 to diffuse turbulently into the exhaust plume. Also shown in Figs. 1–3 are the contributions resulting from neglecting the terms related to the turbulent diffusion.

The change in K_1 does not affect the NO-depletion rate or number density as shown in Fig. 4 because NO is conserved due to the assumptions $NO + NO_2 =$ constant and $NO/NO_2 =$ constant. For small values of K_1 (of the order adopted by the CIAP panel) it is shown[3] that Eq. (1) is effectively independent of turbulence intensity and proceeds at a rate controlled by K_1. It is further pointed out that decreasing K_1 from 0.5 to 0.05 ppm^{-1} sec^{-1} essentially eliminates the "ozone-hole" predicted earlier. The present calculations show that Eq. (1) is quite slow with the small value of $K_1 = 0.6877 \times 10^{-2}$ ppm^{-1} sec^{-1}, and turbulent diffusion can supply most of the O_3 needed to react with NO in the plume.

The calculations presented previously, as well as those reported in Refs. 1 and 3, are based upon the assumption that there is sufficient O available from the photodissociation of NO_2 and O_3 to replenish NO at a rate such that $d(NO)/dt = 0$. This requires that the depletion rate of O be smaller or at most equal to its production rate by photodissociation of NO_2 and O_3. Forming the ratio of these rates, we obtain

$$R = \frac{(\partial O/\partial t)\ \text{Depletion (Hilst)}}{(\partial O/\partial t)\ \text{Photoproduction}} = \frac{K_1[NO][O_3]}{J_3[NO_2] + J_2[O_3]} \qquad (3)$$

where the mixedness term has been dropped in the numerator because it has been shown[3] that the mean value chemistry (see Table 1) can be in error by at most 25%.

Table 1 Values of reaction rate and photodissociation coefficients employed in computations

K_1, ", ", ", K_{15}	Taken from Ref. 2 for $T = 217$ K at 20 km alt
$J_1 = 5.0 \times 10^{-5}$	Ref. 4[a]
$J_2 = 3.0 \times 10^{-4}$	"
$J_3 = 8.0 \times 10^{-3}$	"
$J_4 = 9.0 \times 10^{-5}$	"
$J_5 = 5.0 \times 10^{-7}$	Ref. 4[a]

[a] The values of the photodissociation coefficients are calculated for an average solar zenith angle of 67.5° using observed ozone density distribution at 47°N from Dutsch.[5]

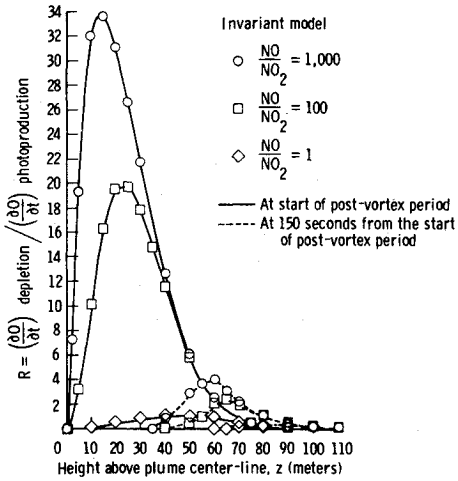

Fig. 5 Variation of the O depletion-to-photo-production ratio computed from plume centerline.

The ratio R, as a function of distance from the plume centerline, is shown in Fig. 5 at the beginning of the post-vortex period ($t = 0$) and 150 sec after the beginning ($t = 150$) for various values of $[NO]/[NO_2]$. The importance of the value $[NO]/[NO_2]$ is evident from this figure. In the calculations of Hilst, et al.,[1,3] the results depend upon the fact that the ratio $[NO]/[NO_2]$ is constant and are independent of the actual value of $[NO]/[NO_2]$. From Fig. 5, it can be seen at $t = 0$ that the depletion rate of O is greater than its rate of production by photodissociation of NO_2 and O_3 for most of the plume except for the case $[NO]/[NO_2] = 1$. A value of $[NO]/[NO_2] = 1$ is probably unrealistic, however, and the number density of NO should be several orders of magnitude larger than that of NO_2.§ If the ratio R is greater than unity, this implies that a deficit of O will occur and the NO cannot be replenished from reaction Eq. (2) at a rate that will maintain a constant NO number density. This result in turn means that the O_3 depletion rate calculated,[1,3] as well as the present calculations (Figs. 1 and 2), are unrealistically high. Similar conclusions can be drawn from Fig. 5 for $t = 150$ sec although values of R are somewhat lower than for the $t = 0$ results. The question of interpretation of the results at $t = 150$ sec is academic at any rate. The $t = 0$ results imply that initially O and NO will be depleted and NO_2 will accumulate. Thus, it is entirely unrealistic to assume the ratio $[NO]/[NO_2]$ to remain constant during the post-vortex period. Subsequent calculations will illustrate this point.

Table 2 Reactions included in the 20-step model

$NO + O_3 \xrightarrow{K_1} NO_2 + O_2$	1
$NO_2 + O(^3P) \xrightarrow{K_2} NO + O_2$	2
$O(^3P) + O_2 + M \xrightarrow{K_3} O_3 + M$	3
$O(^3P) + OH \xrightarrow{K_4} H + O_2$	4
$H + O_2 + M \xrightarrow{K_5} HO_2 + M$	5
$OH + HO_2 \xrightarrow{K_6} H_2O + O_2$	6
$2HO_2 \xrightarrow{K_7} H_2O_2 + O_2$	7
$OH + H_2O_2 \xrightarrow{K_8} H_2O + HO_2$	8
$OH + O_3 \xrightarrow{K_9} HO_2 + O_2$	9
$O(^1D) + H_2O \xrightarrow{K_{10}} 2OH$	10
$NO + HO_2 \xrightarrow{K_{11}} OH + NO_2$	11
$HO_2 + O_3 \xrightarrow{K_{12}} OH + 2O_2$	12
$O(^1D) + M \xrightarrow{K_{13}} O(^3P) + M$	13
$OH + HNO_3 \xrightarrow{K_{14}} H_2O + NO_3$	14
$OH + NO_2 + M \xrightarrow{K_{15}} HNO_3 + M$	15
$O_3 + h\nu \xrightarrow{J_1} O(^1D) + O_2$	16
$O_3 + h\nu \xrightarrow{J_2} O(^3P) + O_2$	17
$NO_2 + h\nu \xrightarrow{J_3} NO + O(^3P)$	18
$H_2O_2 + h\nu \xrightarrow{J_4} 2OH$	19
$HNO_3 + h\nu \xrightarrow{J_5} OH + NO_2$	20

It does not seem entirely unreasonable to consider the plume to be well-mixed after the vortex period. Furthermore, it was shown[3] that the mean value chemistry can be in error at most by 25%. The assumption will also be made that, for short periods of time at the beginning of the post-vortex period, diffusion may be neglected. This so-called "well-mixed plume" analysis is similar to that of Hoshizaki et al.,[6] except for the chemistry model. Simplification of the problem by the foregoing assumptions allows consideration of a more complete chemistry mechanism which, hopefully, will provide some insight into the important reactions and avoid the shortcomings of the two-step model. The reaction mechanism to be considered is given in Table 2.

The net production rate of the various species is then written as

$$\partial[O_3]/\partial t = -K_1[NO][O_3] + K_3[(O^3P)][O_2][M] - K_9[OH][O_3] - K_{12}[HO_2][O_3] - (J_1 + J_2)[O_3] \quad (4)$$

$$\partial[O(^3P)]/\partial t = -K_2[NO_2][O(^3P)] - K_3[O(^3P)][O_2][M] - K_4[O(^3P)][OH] + K_{13}[O(^1D)][M] + J_2[O_3] + J_3[NO_2] \quad (5)$$

$$\partial[O(^1D)]/\partial t = -K_{10}[O(^1D)][H_2O] - K_{13}[O(^1D)][M] + J_1[O_3] \quad (6)$$

$$\partial[NO]/\partial t = -K_1[NO][O_3] + K_2[NO_2][O(^3P)] - K_{11}[NO][HO_2] + J_3[NO_2] \quad (7)$$

$$\partial[NO_2]/\partial t = K_1[NO][O_3] - K_2[NO_2][O(^3P)] + K_{11}[NO][HO_2] - K_{15}[OH][NO_2][M] - J_3[NO_2] + J_5[HNO_3] \quad (8)$$

$$\partial[OH]/\partial t = -K_4[O(^3P)][OH] - K_6[HO_2][OH] - K_8[H_2O_2][OH] - K_9[O_3][OH] + 2K_{10}[O(^1D)][H_2O] + K_{11}[NO][HO_2] + K_{12}[HO_2][O_3] - K_{14}[HNO_3][OH] - K_{15}[OH][NO_2][M] + 2J_4[H_2O_2] + J_5[HNO_3] \quad (9)$$

$$\partial[H]/\partial t = K_4[O(^3P)][OH] - K_5[H][O_2][M] \quad (10)$$

$$\partial[HO_2]/\partial t = K_5[H][O_2][M] - K_6[OH][HO_2] - 2K_7[HO_2]^2 + K_8[OH][H_2O_2] + K_9[OH][O_3] - K_{11}[NO][HO_2] - K_{12}[O_3][HO_2] \quad (11)$$

$$\partial[H_2O_2]/\partial t = K_7[HO_2]^2 - K_8[OH][H_2O_2] \quad (12)$$

$$\partial[H_2O]/\partial t = K_6[OH][HO_2] + K_8[OH][H_2O_2] - K_{10}[O(^1D)][H_2O] + K_{14}[OH][HNO_3] \quad (13)$$

$$\partial[NO_3]/\partial t = K_{14}[OH][HNO_3] \quad (14)$$

$$\partial[HNO_3]/\partial t = -K_{14}[OH][HNO_3] + K_{15}[OH][NO_2][M] - J_5[HNO_3] \quad (15)$$

with $[O_2]$ and $[M]$ assumed constant.

Equations (4–15) have been integrated using the algorithm of Gear[7] utilizing the following range of initial conditions:

§ In private communication, H. Hoshizaki (of Lockheed Palo Alto Research Lab.) indicated that at the beginning of the post-vortex period, a reasonable value of NO/NO_2 ratio would be around 100.

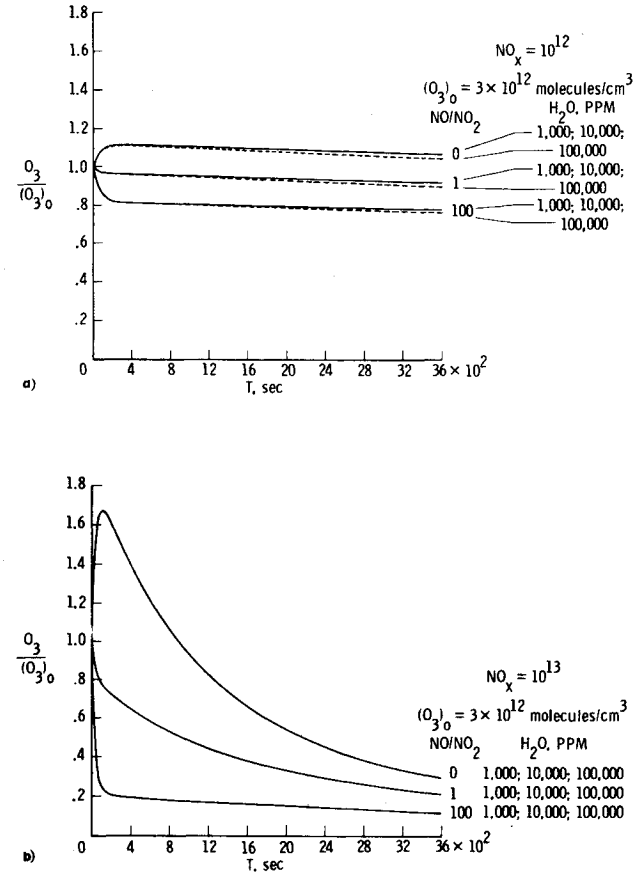

Fig. 6 a) Ozone concentration distribution for the well-mixed case from the start of post-vortex period (total $NO_x = 10^{12}$ molecules/cm^3); b) Ozone concentration distribution for the well-mixed case from the start of post-vortex period (total $NO_x = 10^{13}$ molecules/cm^3).

$[NO+NO_2]_o = 10^{12}$, 10^{13} molecules/cm^3; $[NO/NO_2]_o = 0$, 1, 100; $[O_3]_o = 3\times 10^{12}$, 6×10^{12} molecules/cm^3; $[H_2O]_o = 1000$, 10,000, 100,000 ppm; and $[M] = 2\times 10^{18}$ molecules/cm^3. The integration was arbitrarily carried out for 1 hr. Obviously, for very long times, diffusion should be included, and it is unclear at present how much uncertainty exists in the present calculations due to neglecting the effects of diffusion.

The results of the calculations for $[O_3]_o = 3\times 10^{12}$ particles/cm^3 are presented as a function of time in Figs. 6 and 7. In Fig. 6a, the ratio $[O_3]/[O_3]_o$ is shown as a function of time for $NO_x = 10^{12}$ particles/cm^3. At the end of 1 hr, maximum O_3 depletion of 24% occurs for $[NO/NO_2]_o = 100$ and $[H_2O]_o = 100{,}000$ ppm (3.215×10^{17} particles/cm^3). For $[NO/NO_2]_o = 0$, O_3 is produced initially until the NO concentration builds up above 10^{11} particles/cm^3. Reaction 1 then dominates and causes a net loss of O_3. The depletion of O_3 is only weakly dependent on H_2O concentration for the range investigated. For the highest value, $[H_2O]_o = 100{,}000$ ppm, reaction 9 becomes sufficiently important to contribute to O_3 depletion. Figure 6b indicates similar results for $NO_x = 10^{13}$ particles/cm^3 except that the maximum O_3 depletion is 89%. For this higher initial value of total NO_x, the O_3 kinetics are so dominated by reaction 1 that the results are not affected by the H_2O concentration.

Figures 7a and 7b show the amount of total NO_x converted to HNO_3. For $NO_x = 10^{12}$ particles/cm^3 maximum conversion occurs for $[H_2O]_o = 100{,}000$ ppm. This corresponds to the value for the GE-4 engine at exhaust exit plane.[6] In the post-vortex period, this value will be diluted by one or more orders of magnitude. At the end of 1 hr, 12.5% of the NO_x is present as HNO_3. Conversion of NO_x to HNO_3 is greatest for $[NO/NO_2]_o = 0$ for two reasons; first, because there is initially no NO, very little of the NO_x is involved in the catalytic cycle of reactions one and two; secondly, the larger initial value of NO_2 promotes the effectiveness of reaction 15. For $[H_2O]_o = 10{,}000$ ppm and 1000 ppm, approximately 3% and 1%, respectively, of the NO_x is in the form of HNO_3 after 1 hr. In Fig. 7b, for $NO_x = 10^{13}$ particles/cm^3, the results indicate less than one percent conversion of NO_x to HNO_3 after 1 hr for all cases. Because of the high NO_x concentration, the O_3 is rapidly depleted (see Fig. 6b) and very little $O(^1D)$ is produced. Hence, only an insignificant amount of OH is produced in the critical reaction 10 which is subsequently required in reaction 15 to produce HNO_3.

The results for $[O_3]_o = 6\times 10^{12}$ particles/cm^3 are qualitatively similar. Maximum O_3 depletion occurs for $NO_x = 10^{13}$ particles/cm^3 and $[NO/NO_2]_o = 100$. After 1 hr, 99% of the O_3 has been depleted. Maximum conversion of NO_x to HNO_3 occurs for $NO_x = 10^{12}$ particles/cm^3, $[H_2O]_o = 100{,}000$ ppm and $[NO/NO_2]_o = 0$. For this case, 23% of the NO_x was converted to HNO_3 in 1 hr. For $NO_x = 10^{13}$ particles/cm^3 less than 1% of the NO_x is converted to HNO_3 in 1 hr for all cases.

To summarize the calculations, Figs. 8a and 8b present $[O_3]/[O_3]_o$ and $[HNO_3]/[NO_x]$ as a function of $[H_2O]_o$ at 150 and 3600 sec after the beginning of the post-vortex period. The following observations can be made for the range of variables considered: a) O_3 depletion is only weakly dependent on H_2O concentration; b) O_3 depletion depends strongly on total NO_x concentration and to a lesser degree on initial NO/NO_2 ratio. For NO_x concentrations on the order of 10^{13} particles/cm^3 or greater, much of the O_3 in the post-vortex wake would be destroyed; c) HNO_3 production depends strongly on both H_2O and NO_x concentration. For NO_x concentration of the order of 10^{13} particles/cm^3 an insignificant portion of the

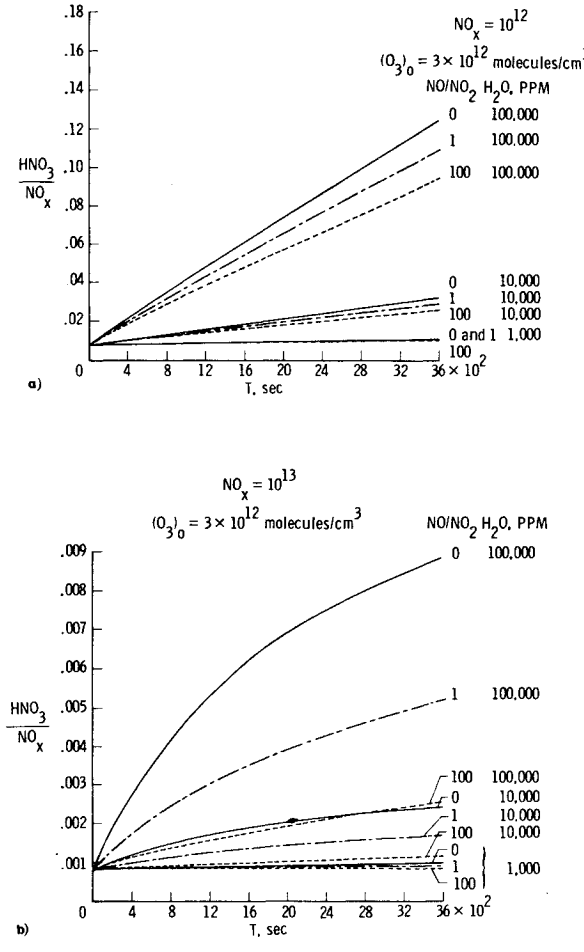

Fig. 7 a) Nitric acid concentration distribution for the well-mixed case from the start of post-vortex period (total $NO_x = 10^{12}$ molecules/cm^3); b) Nitric acid concentration distribution for the well-mixed case from the start of post-vortex period (total $NO_x = 10^{13}$ molecules/cm^3).

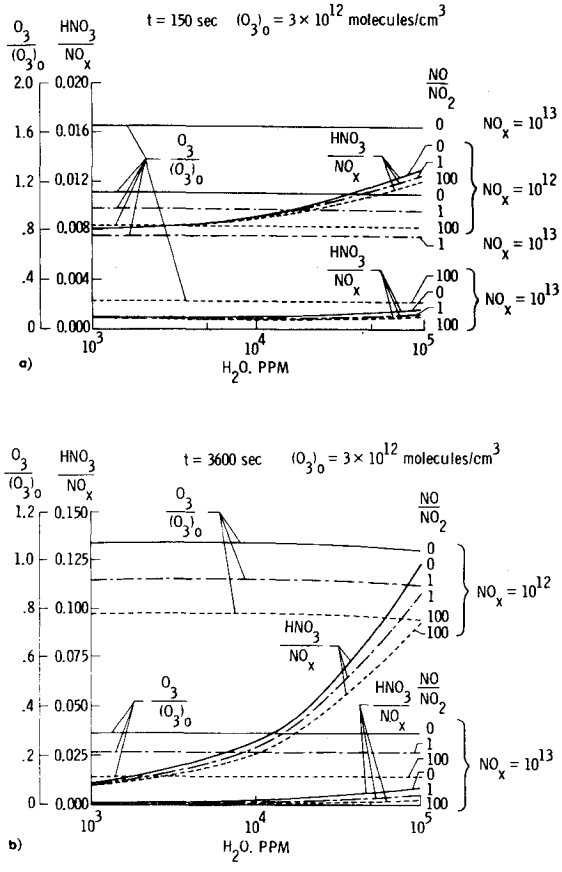

Fig. 8 a) Wake species concentration for the well-mixed case at 150 sec from the start of post-vortex period; b) Wake species concentration for the well-mixed case at 3600 sec from the start of post-vortex period.

NO_x is converted to HNO_3. For NO_x concentrations of the order of 10^{12} particles/cm^3 significant production of HNO_3 occurs only for H_2O concentrations on the order of 100,000 ppm.

Calculations have also been made using a truncated five step reaction model (reactions 1, 2, 3, 17, and 18). Although HNO_3 production is not accounted for in this five-step model, the O_3 depletion results agree within 10% of those predicted by the present 20-step model. A five-step model is attractive because it would permit a coupled chemistry and turbulent diffusion analysis using a second-order closure technique. The coupling is still a formidable task because one needs to solve nine coupled partial differential equations involving the mass fractions and their fluctuations for O_3 and NO, three partial differential equations for NO_x and the same number for the three turbulent fluxes. Obviously, a coupled calculation is required because of the uncertainty introduced in the present analysis by neglecting diffusion.

Conclusions

Calculations of O_3 depletion by NO_x in the exhaust of an SST wake have been made for the following two cases. In the first case, a simplified reaction scheme based solely upon the NO_x catalytic cycle proposed by Hilst et al. has been used. These calculations used reaction rate constants recommended for use by the CIAP chemistry panel. The calculations indicate O_3 depletion in the wake much less severe than that shown in earlier calculations. However, simple analysis indicates that these depletion rates are also too large to be realistic. For most of the wake cross-section, atomic O must be depleted at unrealistically high values (much faster than it can be produced by photodissociation of NO_2 and O_3) to satisfy the restrictive assumption that NO be conserved.

For the second case, the various species are considered to be well-mixed in the wake and diffusion is neglected. These assumptions may be reasonable for short times for the post-vortex period. A more complete chemical reaction scheme has been analyzed. This well-mixed model indicates O_3 depletion in the post-vortex wake is strongly a function of total NO_x and to a lesser degree, a function of initial NO/NO_2 ratio. It, therefore, indicates the importance of determining experimentally total NO_x, NO/NO_2 and the respective distributions of NO and O_3 across the wake before very definite conclusions can be drawn with respect to O_3 depletion. The results also indicate that conversion of significant amounts of NO_x to HNO_3 does not occur except in the presence of very large H_2O concentrations or photolysis rates unrealistically larger than those considered. Based upon present estimates of SST emission, HNO_3 production does not appear to be a factor in reducing the severity of the NO_x catalytic cycle for O_3 destruction.

Appendix A

The various parameters employed in the present computations are briefly described here. The equilibrium turbulence field has been calculated by assuming the following values: a) $\overline{w'^2} = 0.02$ m^2/sec^2; b) mean wind shear, $(\partial\bar{u}/\partial Z)_{\text{mean}} = 10^{-2}$/sec; c) mean temperature lapse rate, $(\partial\bar{T}/\partial Z)_{\text{mean}} = +1°$C/km; d) integral (or computational scale $(\Lambda) = 15$ m; e) $\Lambda/L = 0.55$ (for free turbulent shear flow); where L is the local integral scale length; f) Richardson number, $Ri = 0.1$.

The following assumptions are made regarding the initial distributions of NO and O_3: The NO is assumed to be distributed in the plume in the Gaussian form $\bar{C}_B = \bar{C}_{BO}\exp[-(Z^2/2\sigma^2)]$, with $\sigma = 25$ m and $\bar{C}_{BO} = 2$ ppm. The ozone, O_3, is initially taken as distributed in a complementary Gaussian form with a plume-axis value of zero and an ambient value (outside the plume) of 2 ppm.

References

[1] Hilst, G. R. and Donaldson, C. duP., "The Development and Preliminary Application of an Invariant Coupled Diffusion and Chemistry Model," CR-2295, 1973, NASA; also AIAA Paper 73-101, Washington, D.C., 1973 and Paper 73-535, Denver, Colo., 1973.

[2] Garvin, D. and Hampson, R. F., eds., *Chemical Kinetics Data Survey VII. Tables of Rates and Photochemical Data for Modelling of the Stratosphere (Revised)*, NBSIR 74-430, National Bureau of Standards, Washington, D.C., 1974; supersedes NBSIR 73-203, May 1973.

[3] Hilst, G. R., Donaldson, C. duP., and Contiliano, R., "Some Analyses of the Chemistry and Diffusion of SST Exhaust Materials During Phase III of the Wake Period," CR-132323, 1973, NASA; also presented at the First Special Assembly of the International Association of Meteorology and Atmosphere Physics (IAMAP), Jan. 1974, Melborne, Australia.

[4] Shimazaki, T. and Ogawa, T., "On the Theoretical Model of Vertical Distributions of Minor Neutral Constituents Concentrations in the Stratosphere," Tech. Memo. ERL-OD 20, 1974, NOAA, Boulder, Colo.

[5] Dütsch, H. U., "Photochemistry of Atmospheric Ozone," *Advances in Geophysics*, Vol. 15, 1971.

[6] Hoshizaki, H., et al., "Study of High-Altitude Aircraft Wake Dynamics," Rept. DOT-TST-90-3, Dec. 1972, Dept. of Transportation, Washington, D.C.

[7] Gear, C. W., "The Automatic Integration of Stiff Ordinary Differential Equations," *Proceedings of the International Federation of Information Processing Congress*, Humanities Press, 1968, p. A-81.